



Science Arts & Métiers (SAM)

is an open access repository that collects the work of Arts et Métiers Institute of Technology researchers and makes it freely available over the web where possible.

This is an author-deposited version published in: <https://sam.ensam.eu>
Handle ID: <http://hdl.handle.net/10985/25466>

To cite this version :

Michaël PEREIRA, Nader ZIRAK, Mohammadali SHIRINBAYAN, Grzegorz ZYWICA, Abbas TCHARKHTCHI - Design, fabrication, and evaluation of a small turbine blade manufactured by rotational molding - The International Journal of Advanced Manufacturing Technology - Vol. 128, n°7-8, p.3441-3450 - 2023

Any correspondence concerning this service should be sent to the repository

Administrator : scienceouverte@ensam.eu



Design, fabrication, and evaluation of a small turbine blade manufactured by rotational molding

Michaël Pereira¹ · Nader Zirak^{1,2} · Mohammadali Shirinbayan² · Grzegorz Zywnica³ · Abbas Tcharkhtchi²

Abstract

The notion of renewable energy has become deeply ingrained in the world, captivating an increasing number of researchers and industry professionals who invest substantial resources to advance the development of more efficient systems. While large-scale wind turbine blades currently reach lengths exceeding 50 m and are typically manufactured as single entities, this study focuses on the design and evaluation of a blade profile tailored specifically for small turbines. The blades were manufactured using rotational molding, employing various groups of polymers including thermosets and thermoplastics. To enhance their mechanical performance, foams were incorporated into the polyurethane and polyethylene blades. The suitable blade by evaluating various formulations and foams was identified by mechanical analysis. Aerodynamic analysis was conducted across different ranges of wind speeds and pitch angles. The results indicate that the power coefficient (C_p) closely approaches 0.5.

Keywords Small wind turbine · Polymers · Rotational molding · Performance

1 Introduction

Wind-generated electricity generates no CO₂ emissions and therefore does not contribute to the greenhouse effect. In remote areas or areas with weak power grids, wind power can be used to charge batteries or combined with a diesel engine to save fuel through wind power. In addition, wind turbines can be used for water desalination in coastal areas with little fresh water, for example, in the Middle East. In windy locations, electricity costs, measured in \$/kWh, are competitive with generation costs from conventional methods, such as coal-fired power plants [1–5].

Small wind turbines have been designed with a capacity of up to 100 kW [6], with the most common sizes being between 1 and 10 kW [7, 8]. Considering some advantages of this turbine, such as low installation cost, suitability for

low wind speed areas, better-decentralized power generation, and aesthetically pleasing have turned into good competitors for large turbines [9, 10].

The technical aspect of designing a small wind turbine involves addressing the challenge of achieving a high system efficiency while balancing the need for a straightforward mechanical structure and a cost-effective production process, ultimately resulting in affordable prices. Small wind turbines possess unique characteristics specific to their field of application, and the design process must consider these factors to optimize efficiency both technically and economically [11, 12]. Freere et al. [13] conducted a study on the MG4520, a low-cost wind turbine. In a wind tunnel, a three-blade turbine with a rotor diameter of 2.1 m was tested up to a wind speed of 13 m/s. Blade properties were defined based on wind speed, yaw angle, and whether or not a nose cone was used. At different wind speeds, the researchers found that the values of the tip speed ratio (TSR) varied from 2 to 8 and that the maximum C_p of 0.2 was reached for a TSR of 6, in addition to the fact that no significant change in blade power output was observed with the presence of the nose cone. Overall, the study implies that substantial gains in blade performance are possible, but to avoid turbine stall, the controller and generator would need to be tuned. Singh et al. [14] fitted a 400-W Air-x marine wind turbine with an A2 bladed rotor tested and optimized for low

✉ Nader Zirak
naderzirak23@gmail.com

¹ Arts et Métiers Institute of Technology, CNAM, LIFSE, HESAM University, F-75013 Paris, France

² Arts et Métiers Institute of Technology, CNAM, PIMM, HESAM University, F-75013 Paris, France

³ Institute of Fluid Flow Machinery, Polish Academy of Sciences, Fiszerka 14, 80-231, Gdansk, Poland

reapplication (1.26 m diameter). For better aerodynamic performance at low wind speeds, the rotor had an exponential distribution of torsion and taper along with the AF300 airfoil. The aerodynamic performance of a four-bladed wind turbine with a 500-mm diameter rotor and a National Advisory Committee for Aeronautics (NACA) 2404 wing profile was tested at 15, 18, and 20° bank angles and low wind speeds. They compared the performance of the air-performance X with a 2-blade rotor to that of a 3-blade rotor (rotor diameter 1.16m): In the low wind speed range of 3–7 m/s, two-bladed rotors were found to have better C_p . The two-bladed rotor is supplied more than twice as much power as the basic rotor at the optimum pitch of 18°.

Turbine blades have been manufactured with different methods such as rotational modeling [15], hand lay-up [16], vacuum infusion [17], pre-preg [18], injection molding [19], and 3D printing methods [4]. Considering the advantages of rotational molding compared to the other mentioned methods of fabrication as an automated process that requires less manual labor and skill, produces large, hollow shapes with complex geometries, a low-pressure process that does not require the use of expensive molds or tooling, produces parts with low levels of residual stress and can be used with a wider range of materials [20], has made it a suitable method for producing small turbine blades. Rotational molding, also referred to as rotomolding, is a versatile technique for manufacturing hollow parts with varying sizes and complexities, eliminating the need for additional welding or assembly [21]. When compared to other plastic transformation methods, rotational molding stands out for its straightforward and relatively clean process [22]. The origins of this technique can be traced back to the 1930s when the first rotational molding machines were developed. The introduction of plastisols, specifically PVC, by Union Carbide in the 1940s, and the subsequent advent of high-quality thermoplastics like polyethylene in the 1950s and 1960s, played a pivotal role in the widespread adoption of rotational molding. Notably, the toy industry became a significant proponent of rotational molding during this period, capitalizing on the advantageous properties of PVC and polyethylene [23, 24].

The novel application of rotational molding to the blade manufacturing strategy of small wind turbines with low-cost, large-scale production potential has been studied [15, 25]. However, reinforcing the blades with fibers and metal insert has been considered necessary which requires time and cost. This study focuses on the design and evaluation of a small turbine blade profile specifically tailored for rotational molding. Improving the mechanical properties was investigated by incorporating foam in the polymeric blades as a quick and economical method with polyurethane and polyethylene foams which provide two different types of close and open cells foam, respectively. That, a lightweight blade can be manufactured along with increasing the mechanical properties which is an

important criterion for fabrication the blades. In addition, different polymer materials, including thermosets (various formulations of polyurethanes) and polyethylene, have been inquired. The selection of suitably fabricated blades was conducted by mechanical analysis. Finally, aerodynamic analysis was performed at various wind speeds, and pitch angles to analyze the performance of manufactured turbine blades. The results show improvement in the mechanical properties of foamed blades with good potential for manufacturing small wind turbine blades with a C_p closely approaching 0.5.

2 Blade design, manufacturing, and characterization

2.1 Design

The blade was designed to function in an operating range of wind speeds from 8 to 14 m/s with rotational speeds up to 500 rpm. The nominal power is considered 1 kW for a wind speed of 15 m/s. Regarding the airfoil design, NACA 2415 was selected for this study. Analysis of this profile design for low wind speed conditions showed a 50-W generation with wind speeds below 5 m/s [26]. The wind turbine is placed in a space swept by air of speed V_1 upstream, of speed V in the plane of the propeller, and of speed V_2 downstream of the propeller plane. The geometry of the rotor can be simplified to its diameter D , its swept surface ($S = \pi D^2/4$), its energy recovery capacity, its axial thrust F , its moment M , and its mechanical power $P = M\omega$. Upstream of the disc swept by the wind turbine, the pressure is higher than downstream. This pressure difference is the source of the force exerted by the wind on the wind turbine. The diameter of the wind turbine for a wind speed of 14 m/s through Froude-Rankine theory was achieved at 1.70 m. After that, the optimal value for the chord at the end, chord at the base, pitch angle, and rotational speed were defined as 0.1, 0.24, 5°, and 500 rpm, respectively.

2.2 Manufacturing

2.2.1 Materials

Polyurethane (PU) and polyethylene (PE) were the thermoset and thermoplastic groups, respectively, that have been evaluated to fabricate the blades. Rotational molding was carried out in two stages by LIM and RAIGI with LIM resources (rotational molding machine and mold). The polyurethane used for fabrication was a grade commercial product under the product code ICORENE 4-35150. Regarding polyurethane roto molding, the grades used are commercial grades from RAIGI: Gyrothane 900/Raigidur FPG (yellow blades) and Gyrothane 919/Raigidur DDG (black blades). Different colors were used to visually distinguish the two grades. The reagents are stored

at a temperature slightly below 20 °C, then mixed manually in the appropriate proportions; the mixture is then poured into the mold before it is rotated. The mold was previously covered with a release agent (DE8340). The rotational molding conditions are 5 min at room temperature, 10 min at 80 °C, then 15 min of cooling for demolding at around 35–40 °C.

In order to achieve optimal mechanical performance, the blades were foamed. For each type of PU and PE body, two different foams of PU and PE were applied. PU foam was injected into both body types, while PE foam was used for the PE blade. Two PU foam formulations were used with different free densities:

- (i) Raigithane 20643/Raigidur TR with a free density of 41 g/l.
- (ii) Raigithane 20607-2/Raigidur TR with a free density of 85 g/l.

These 2 foams were injected into the 3 hollow blade types. It was the rotational molding mold that served as a shaper. The quantities of foam injected into the skin are around 200 g for the densest PU foam (R20607-2/TR) and around 120 g for the least dense PU foam (R20643/TR). In the case of PE foaming, the PE blades have not only been filled with PU foam, but they have also been filled with PE foam. It is a commercial PE foam (Revolve M-644 from Matrix).

- (i) The principle of PE foaming: A foam is a cellular material made up of a polymer matrix and gas bubbles. From a general point of view, foam is the result of the expansion of gas cells in a molten polymer. This gas is obtained from foaming agents of two different types:
- (ii) Physical blowing agent: volatile liquid (hydrocarbons, CFCs, water, etc.), permanent gas (mainly CO₂).

Chemical blowing agent (usually available in powder form), which decomposes under the effect of heat and releases gaseous substances. A cell is a volume of gas surrounded by a certain amount of molten polymer. If the percentage of the blowing agent (the amount of gas produced) is very low, the number of bubbles and the volume fraction of the gas will remain low. Bubbles in the final state will remain spherical.

Two types of foam can be distinguished: open-cell foam and closed-cell foam (the cells are separated by thin layers of polymers (Fig. 1)).

It can be noted that the rotational molding conditions of the skins are different from those presented in the previous paragraph. Indeed, the body formed would not withstand the foaming conditions without degrading. The temperatures and duration of such exposure will deteriorate the blades. This is why, when the blades are rotomoulded and then foamed, the rotational molding cycle is shorter and we take advantage of the foaming and its heat to finish the skin (distribution of the material). It can be noted that PE foam is much denser; the weight of the added foam is around 260 g.

2.2.2 Rotational molding procedure

According to the geometry of the blade, a mold through the machining of two aluminum blocks was fabricated (Fig. 2). The mold was filled from its end part, and considering the geometry, the centrifugal effect was enough to feed the polymer mold at this position. Rotational modeling under the “LAB 40” brand was used to manufacture the blades. The process parameters, such as oven temperature, rotational speeds, and heating and cooling rates, were controlled through a computer interface.

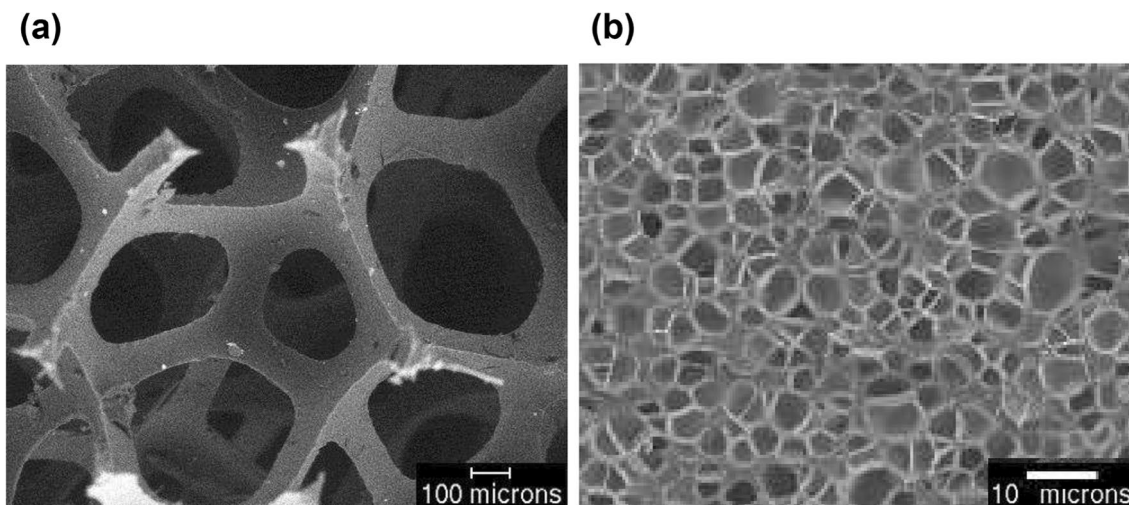


Fig. 1 Scanning electron microscopy of different cell foams: **a** open cell foam of PU and **b** closed cell foam of PE

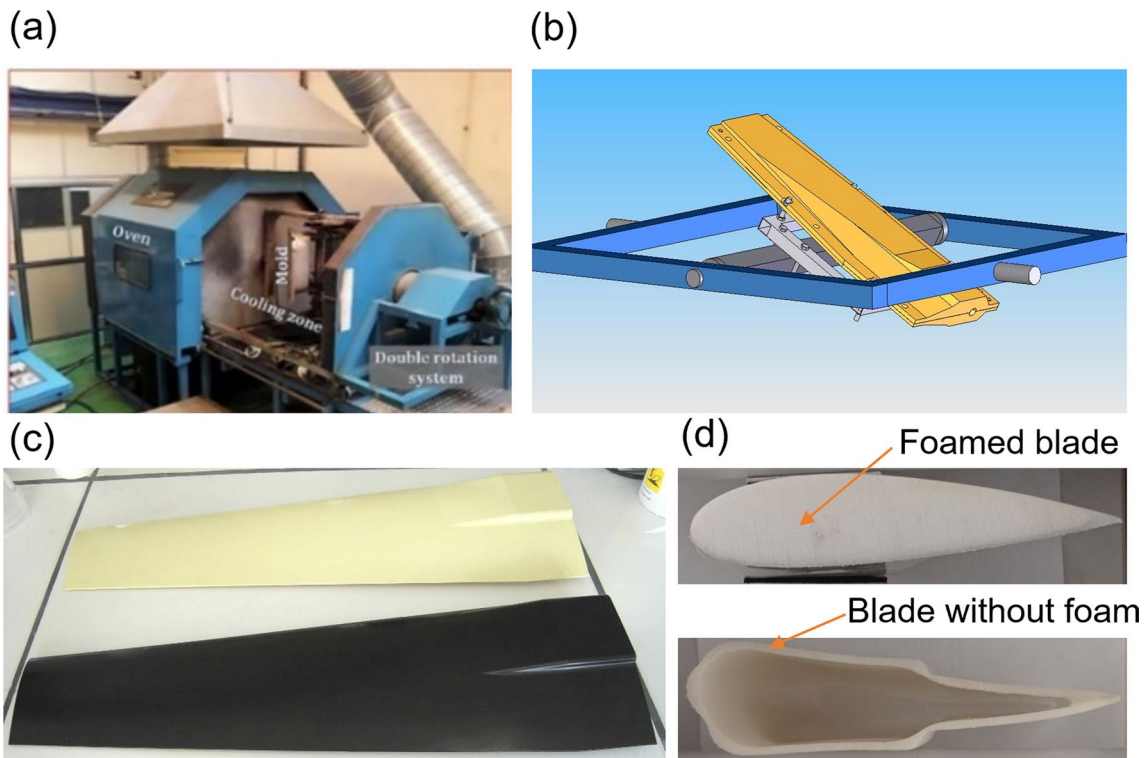


Fig. 2 **a** Rotational molding machine LAB 40, **b** assembled design of the mold, **c** rotationally molded polyurethane wind turbine blades, and **d** view of cross-section cut of wings with and without foam

2.3 Test bench

The test section is followed by a convergent two series of 90° bends which direct the air towards the return channel. A screen is installed at the entrance to the return channel to ensure a certain homogenization of the flow, which remains however very turbulent due to the bends that precede the channel.

The channel is specially designed to test wind turbine rotors, where the presence of flow turbulence is inconsequential due to the requirement for wind turbines to function efficiently under substantial atmospheric turbulence conditions. The length of the channel is about 10 m, and its section is square with a side of 3 m. Given its large section, 4 times greater than that of the test section, the wind speed in the return channel can reach up to 10 m/s.

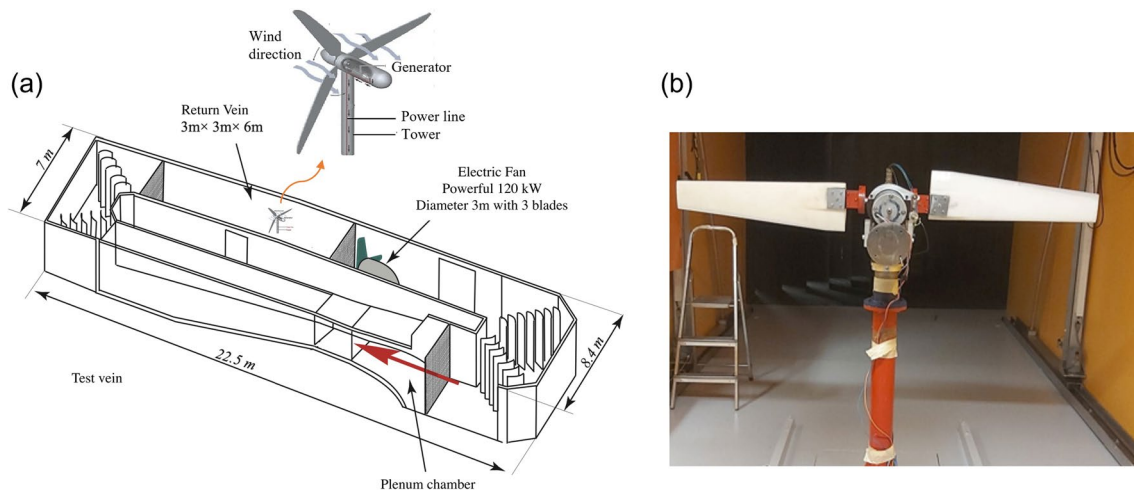


Fig. 3 **a** 3D plan of the wind tunnel and **b** a view of test vein section in the wind tunnel test



Fig. 4 Bending test on the blades

The wind turbine is installed in the return channel of the wind tunnel and tested under the effect of a known and controlled wind speed (Fig. 3). The blades manufactured by rotational molding are equipped with specific inserts allowing them to be mounted on the instrumented nacelle already installed in the wind tunnel for testing wind turbine rotors. A tachometric generator (Radio Energie — type RN 0522) allows the measurement of the speed of rotation of the wind turbine and operates as needed as a generator or motor. An electromagnetic powder brake (FBB — type 3) allows, from an adjustable electrical intensity, to apply a resistive torque on the shaft of the wind turbine and absorbs the power produced by the wind turbine in the transforming into heat. Thus, the wind turbine can be studied under different

load conditions. A rigid arm fitted with a dynamometer (SEDEME type AC 50 daN, no. 4490) is powered by an extensometer bridge. This arm secures the brake stator to the frame with a known eccentricity relative to the axis of rotation of the wind turbine. Thus, the torque applied by the brake is translated into a force that can be measured with the dynamometer.

2.4 Characterization methods

For analyzing the mechanical properties, quasistatic tensile tests were performed by using the MTS 830 hydraulic machine with a loading cell of 10 kN at a constant ramp speed of 5 mm/min. At least four repetitions were performed

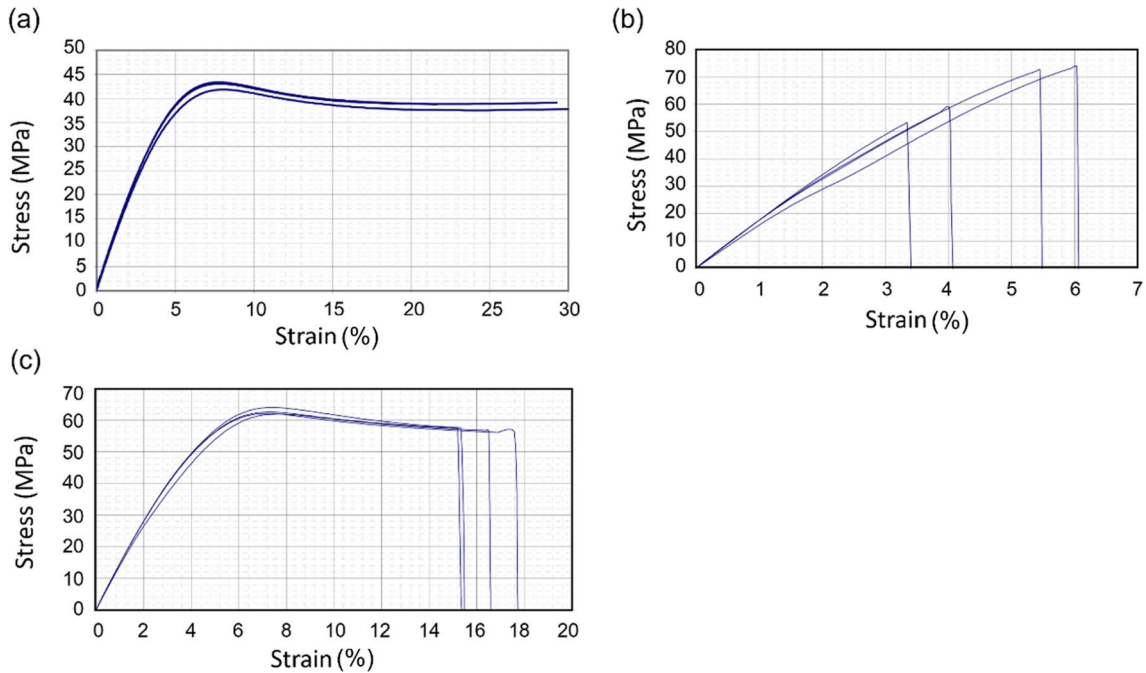


Fig. 5 Stress-strain curves from different formulas of PU: **a** formulation 1, **b** formulation 2, and **c** formulation 3

Table 1 Results from tensile tests for different formulations of samples

Sample	E (MPa)	σ_{\max} (MPa)	ϵ_{\max} (%)	Elongation at break (mm)	Force at break (kN)	σ_f (MPa)	ϵ_f (%)
Formulation 1	1012.00	42.97	35.98	14.23	1.09	39.11	23.72
Formulation 2	1731.53	65.00	4.75	2.83	1.85	65.00	4.73
Formulation 3	1470.31	62.72	16.29	9.75	1.77	56.89	16.25

for each tensile test, and the average of the results was finally reported. The PU was supplied by Raigi company in 3 batches of 8 specimens [27]. In each of these 3 batches, there are 4 tensile specimens and 4 bending specimens; each one is identified by the letter F or T followed by its identifying number (1 to 4). Each test will be carried out at room temperature (23 °C). The different PU formulation has been named commercially as follows by Raigi company:

Formulation 1: Gyrothane 900 + Raigidur FPG [28],

Formulation 2: Gyrothane FR0403 + Raigidur F and

Formulation 3: Gyrothane 919 + Raigidur DDG.

Bending tests were carried out on the blades (Fig. 4). This test was developed by the Raigi laboratory in order to compare the behavior of the blades together. The blades were fixed on a metal frame at a fixed distance from a spherical

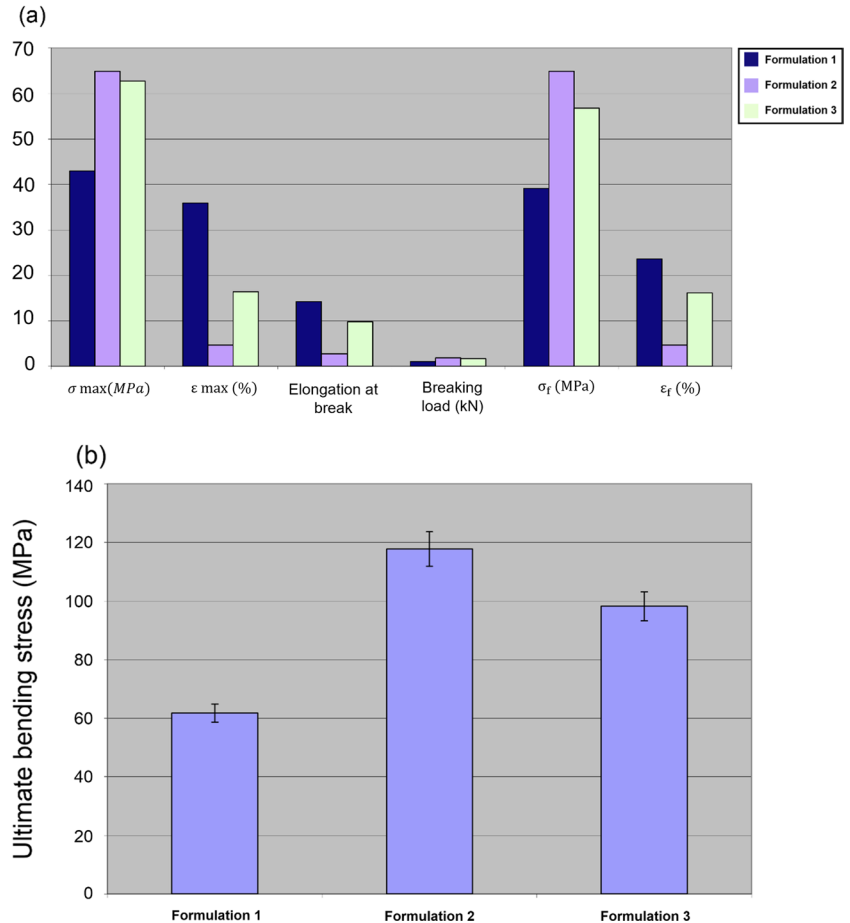
indenter. The test consists of bending the blade under the effect of the indenter at a fixed distance by measuring the displacement of the indenter and the associated force at each instant. In order not to cause the blades to crack or be destroyed before the wind tunnel tests, the maximum distance for movement of the indenter has been set at 19 mm.

3 Results and discussion

3.1 Tensile and flexion behavior

Figure 5 shows the stress (MPa)–strain (%) curves obtained from the tensile tests on PU. Young's modulus is determined from the slope of the tangent at the origin of this curve. The

Fig. 6 **a** Results from tensile tests and **b** ultimate bending stress for the samples with different formulation



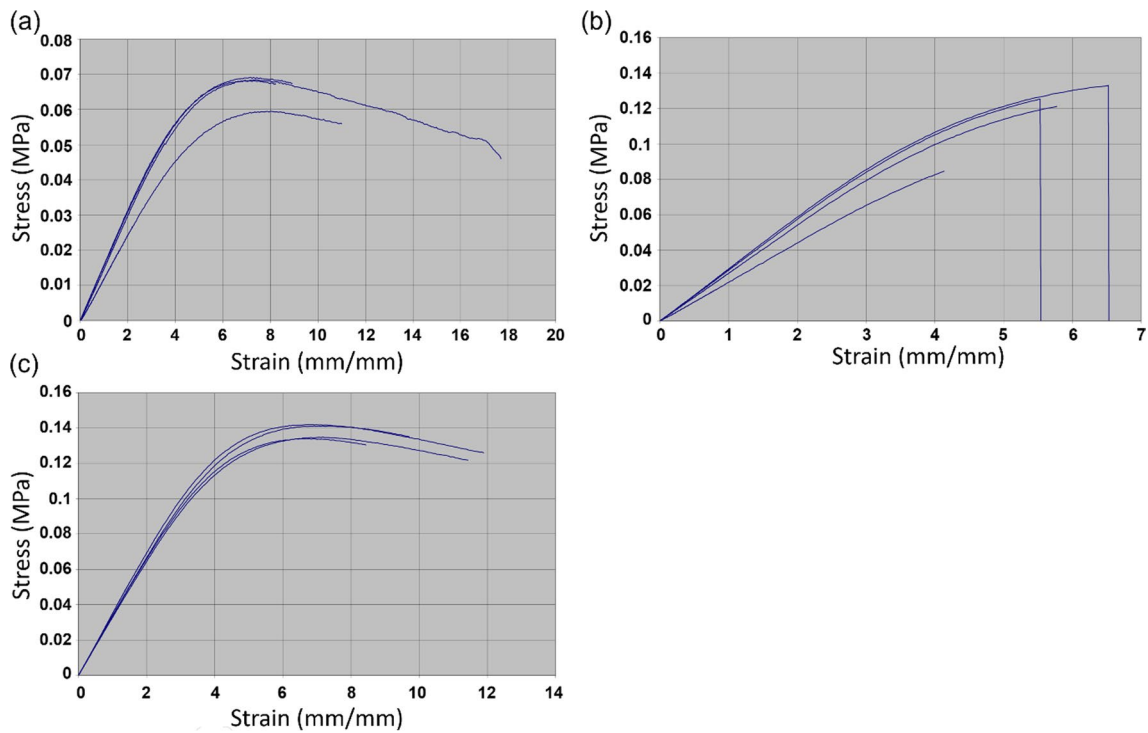


Fig. 7 Curves of bending test for different formulations: **a** formula 1, **b** formula 2, and **c** formula 3

modulus values are calculated between 0.0025 and 0.005% deformation according to the standard. Other parameters determined are stress and strain at failure and maximum stress and strain. The results are summarized in Table 1.

According to the results, the presence of defects in specimens causes a slight dispersion, in particular for deformation. Also, it is observed that there are two ranges of materials among the 3 formulations studied: two formulations (formulations 1 and 3) with an elongation of a few tens of percent and one formulation (formulation 2) much less deformable (Fig. 6).

On the other hand, formulations 1, 2, and 3 do not appear to us to have a fragile behavior. However, the maximum stress and the breaking stress of formulations 1 and 3 are a little below formulation 2. Regarding tensile modulus, materials are classified as Formulation 1 < Formulation 3 < Formulation 2.

Figure 7 shows the load (kN)–displacement (mm) curves obtained by bending tests on PU. After performing the various tests on three polyurethane formulations, it appears that formulations 1 and 3 correspond best to the application. The materials selected for rotational molding of wind turbine blades

Table 2 Results of force from the different displacement of the blades in the flexion mode

Blade code	Body material	Foam	Force caused by displacement of 2 mm	Force caused by displacement of 5 mm	Force caused by displacement of 7 mm	Force caused by displacement of 10 mm	Force caused by displacement of 15 mm	Force caused by displacement of 19 mm
1	G900/FPG	-	6.56	15.64	21.63	30.63	45.17	55.89
2	G919/DDG	-	7.93	19.68	27.01	38.68	56.92	71.11
3	PE	-	2.06	4.77	6.37	8.54	11.9	14.42
4	G900/FPG	20607-2	9.58	22.81	31.7	44.98	66.95	83.62
5	G900/FPG	20643/TR	8.54	21.82	30.44	43.45	64.81	81.02
6	G919/DDG	20607-2/TR	10.22	26.7	37.27	53.6	79.35	98.72
7	G919/DDG	20643/TR	10.3	25.98	36.16	51.92	76.83	97.24
8	PE	20607-2	3.74	8.54	11.71	16.25	23.31	28.46
9	PE	20643/TR	3.7	8.58	11.56	15.95	22.7	27.81
10	PE	PE	2.29	5.49	7.29	9.88	14.27	17.51

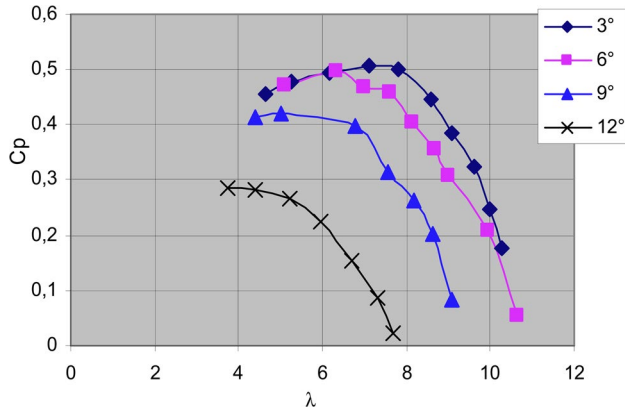


Fig. 8 The power of the wind turbine against a specific speed

are Formulation 1: Gyrothane 900 + Raigidur FPG (yellow blades) and Formulation 3: Gyrothane 919 + Raigidur DDG (black blades).

3.2 Mechanical analysis of the blades

Damage resulting from bending loads, generated by aerodynamic and gravity forces, is a common occurrence in wind turbines [29]. In this section, the suitable blade by evaluating various formulations and foams has been identified by measurement of the forces exerted by a specified displacement of the blades. The results with respect to the different blades

and specific displacement from 2 to 19 mm are presented in Table 2. According to the results, the foaming has a positive effect on the bending resistance of the blades. The variations in the resistance values to bending of blades in PE (blades code 8, 9, and 10) are much weaker compared to PU in absolute value. However, foaming showed a mechanical improvement on the PE blades. The two polyurethane foams have a similar effect on the characteristics of the blades, but the foam with the least dense (R20643/TR) will be more interesting for the production of blades because it makes it possible to produce the lightest possible blades with identical properties.

4 Field testing

The wind turbine tests with rotomolded blades (blades 6 and 7, PU foamed PU blades) are carried out under the following conditions. The rotation speed of the wind turbine is limited to around 500 rpm to avoid the risk of tearing off the blades at the level of the inserts by the effect of centrifugal force. Four-blade pitch angles 3°, 6°, 9°, and 12° are tested in order to define their influence on the energy performance of the wind turbine.

The wind speed is kept constant for each setting, and a resistive load is applied to the wind turbine shaft. This load is ensured using the electric powder brake, and its value is varied until the rotor is completely blocked. The mechanical power developed on the wind turbine shaft is determined by the torque and the rotation speed measured.

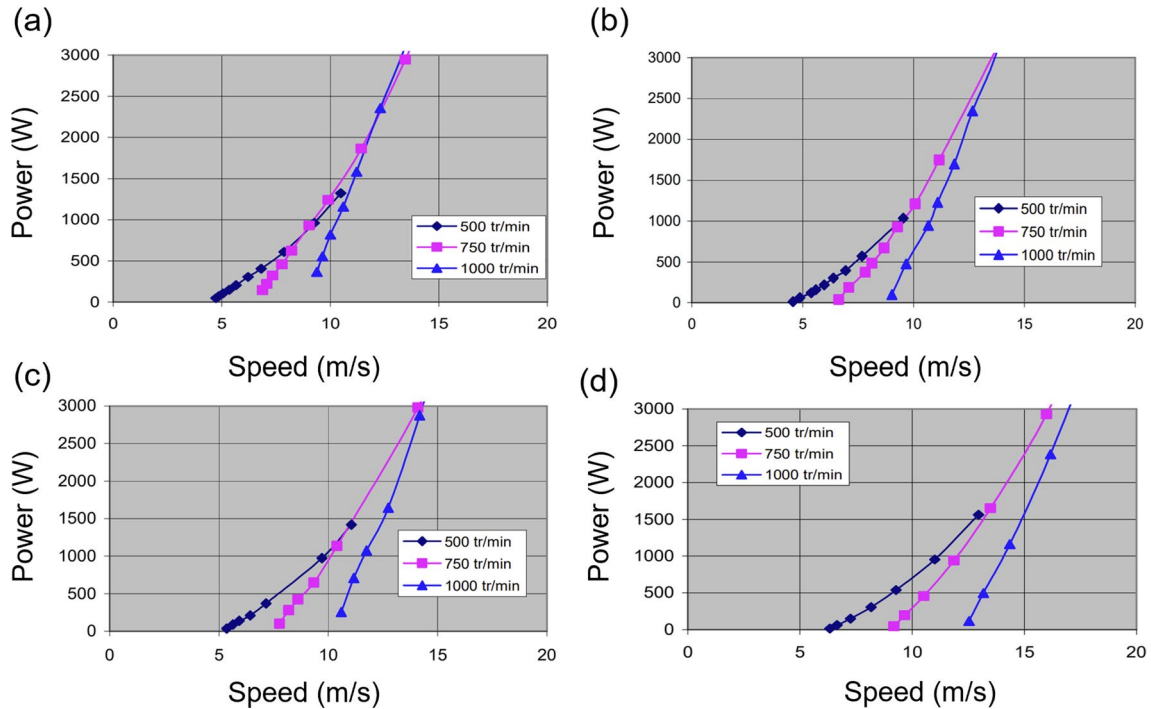


Fig. 9 Power against the wind speed at 3 constant rotation speeds of the turbine shaft a 3°, b 6°, c 9°, and d 12°

The results are presented in the dimensionless form wind turbine power coefficient C_p as a function of its specific speed λ (Fig. 8).

The results presented in the following four figures (Fig. 9) can be established. Each curve concerns a set angle and operation of the wind turbine at 3 constant rotation speeds $N = 500$ rpm, 750 rpm, and 1000 rpm. From these curves, one can predict the energy production as a function of the wind speed for each regulation of the rotational speed of the rotor. For example, a power of 1 kW can be obtained with a wind of about 9.4 m/s when the pitch angle is 3° and the rotation speed is 500–750 rpm.

5 Conclusions and further directions

This study concerns the wind tunnel tests and the characterization of the operation of a wind turbine 1750 mm in diameter, equipped with two straight blades manufactured by rotational molding. The performance of the wind turbine is studied at different blade pitch angles 3° , 6° , 9° , and 12° . The results are presented on the one hand in the form of adimensional parameters: power coefficient according to the specific speed of the wind turbine $C_p = f(\lambda)$. On the other hand, the results are presented in the form of power curves as a function of the wind speed for 3 values of regulation of the rotation speed of the rotor $N = 500$ rpm, 750 rpm, and 1000 rpm. In terms of aerodynamics and energy, the wind tunnel tests show that the wind turbine tested can achieve excellent performance. Indeed, its power coefficient C_p is close to 0.5 for a blade pitch angle of 3 to 12° . It should be remembered that the maximum theoretical yield defined by Betz's law is $C_p = 0.59$. The work carried out makes it possible to demonstrate the feasibility of producing small wind turbines with rotationally molded blades. Future research directions for this study involve optimizing the rotational molding process parameters and design technology. This includes incorporating advanced design features using structural analysis and experimental evaluations. These research directions aim to improve the efficiency, durability, and cost-effectiveness of turbine blades manufactured by rotational molding and provide valuable insights for the industry.

Author contributions Michaël Pereira: investigation, writing—original draft, writing—review and editing; Nader Zirak: conceptualization, investigation, writing—original draft, writing—review and editing; Mohammadali Shirinbayan: conceptualization, writing—original draft, editing; Grzegorz Żywica: conceptualization, writing—review and editing; Abbas Tcharkhtchi: project administration, supervision, visualization, conceptualization, editing.

Data Availability The raw/processed data required to reproduce these findings will be made available on request.

Declarations

Ethics approval The authors are obliged to all the rules regarding the ethics in publication.

Consent to participate This study is not a human transplantation study. No consent is needed for this paper.

Consent for publication The authors consent to the policy of publication in The International Journal of Advanced Manufacturing Technology.

Competing interests The authors declare no competing interests.

References

- Kim K, Kim H-G, Kim C, Paek I, Bottasso CL, Campagnolo F (2018) Design and validation of demanded power point tracking control algorithm of wind turbine. *Int J Precis Eng Manuf Technol* 5:387–400
- Bhandari B, Poudel SR, Lee K-T, Ahn S-H (2014) Mathematical modeling of hybrid renewable energy system: A review on small hydro-solar-wind power generation. *Int J Precis Eng Manuf Technol Springer* 1:157–173
- Carre A (2019) Miniaturisation bioinspirée d'un convertisseur aéromécanique pour l'exploitation des faibles vitesses de vent. Université Grenoble Alpes (ComUE)
- Rouway M, Nachtane M, Tarfaoui M, Chakhchaoui N, Omari LEH, Fraija F et al (2021) 3D printing: Rapid manufacturing of a new small-scale tidal turbine blade. *Int J Adv Manuf Technol* 115:61–76
- Bukala J, Damaziak K, Karimi HR, Malachowski J, Robbersmyr KG (2019) Evolutionary computing methodology for small wind turbine supporting structures. *Int J Adv Manuf Technol* 100:2741–2752
- Kim K, Kim H-G, Paek I (2020) Application and validation of peak shaving to improve performance of a 100 kW wind turbine. *Int J Precis Eng Manuf Technol Springer* 7:411–421
- Simic Z, Havelka JG, Vrhovcak MB (2013) Small wind turbines—a unique segment of the wind power market. *Renew Energy* 50:1027–1036
- Lim CW (2017) Design and manufacture of small-scale wind turbine simulator to emulate torque response of MW wind turbine. *Int J Precis Eng Manuf Technol Springer* 4:409–418
- Karthikeyan N, Murugavel KK, Kumar SA, Rajakumar S (2015) Review of aerodynamic developments on small horizontal axis wind turbine blade. *Renew Sustain Energy Rev* 42:801–822
- Kumar PM, Sivalingam K, Narasimalu S, Lim T-C, Ramakrishna S, Wei H (2019) A review on the evolution of Darrieus vertical axis wind turbine: Small wind turbines. *J Power Energy Eng* 7:27–44
- Scappatici L, Bartolini N, Castellani F, Astolfi D, Garinei A, Pennicchi M (2016) Optimizing the design of horizontal-axis small wind turbines: from the laboratory to market. *J Wind Eng Ind Aerodyn* 154:58–68
- Song Q, David LW (2014) Design and testing of a new small wind turbine blade. *J Sol energy Eng. American Society of Mechanical Engineers* 136:34502
- Freere P, Sacher M, Derricott J, Hanson B (2010) A low cost wind turbine and blade performance. *Wind Eng*, vol 34. SAGE Publications Sage, UK: London, England, pp 289–302
- Singh RK, Ahmed MR (2013) Blade design and performance testing of a small wind turbine rotor for low wind speed applications. *Renew Energy* 50:812–819

15. Marrero MD, Hernández P, Suárez L, Pestana D, Benítez A, Martín J et al (2014) Rotational molding applied to the manufacturing of blades of small wind turbine. *Eng Syst Des Anal* 45851:V003T14A014
16. Cairns D, Skramstad J, Mandell J (2001) Evaluation of hand lay-up and resin transfer molding in composite wind turbine blade structures. In: 20th 2001 ASME Wind Energy Symp, p 24
17. Hunter-Alarcon RA, Leyrer J, Leal E, Vizan A, Perez J, Da Silva LFM (2018) Influence of dissimilar composite adherends on the mechanical adhesion of bonded joints for small blade wind turbine applications. *Int J Adhes Adhes* 83:178–183
18. Katnam KB, Comer AJ, Roy D, Da Silva LFM, Young TM (2015) Composite repair in wind turbine blades: an overview. *J Adhes Dent* 91:113–139
19. Kim B, Park S-J, Ahn S, Kim M-G, Yang H-G, Ji H-S (2021) Numerically and experimentally verified design of a small wind turbine with injection molded blade. *Processes* 9:776
20. Crawford RJ (2012) Practical guide to rotational moulding. *Smithers Rapra*
21. Gupta N, Ramkumar PL, Sangani V (2020) An approach toward augmenting materials, additives, processability and parameterization in rotational molding: a review. *Mater Manuf Process* 35:1539–1556
22. Nugent P (2006) Rotational molding. *Handb Plast Process*. Wiley Online Library, pp 387–453
23. León LDVE, Escocio VA, Visconte LLY, Junior JCJ, Pacheco EBAV (2020) Rotomolding and polyethylene composites with rotomolded lignocellulosic materials: a review. *J Reinf Plast Compos*, vol 39. SAGE Publications Sage, UK: London, England, pp 459–472
24. Evode N, Qamar SA, Bilal M, Barceló D, Iqbal HMN (2021) Plastic waste and its management strategies for environmental sustainability. *Case Stud Chem Environ Eng* 4:100142
25. Van der Walt JL (2020) Development of a cost efficient wind turbine blade for low wind speeds. North-West University (South Africa)
26. Vilar AÁ, Xydis G, Nanaki EA (2020) Small wind: a review of challenges and opportunities. In: *Sustain Resour Tomorrow*. Springer, pp 185–204
27. Tcharkhtchi A, Farzaneh S, Abdallah-Elhirsy S, Esmaeillou B, Nony F, Baron A (2014) Thermal aging effect on mechanical properties of polyurethane. *Int J Polym Anal Charact Taylor & Francis* 19:571–584
28. Farzaneh S, Riviere S, Tcharkhtchi A (2012) Rheokinetic of polyurethane crosslinking time-temperature-transformation diagram for rotational molding. *J Appl Polym Sci* 125:1559–1566
29. Ullah H, Ullah B, Silberschmidt VV (2020) Structural integrity analysis and damage assessment of a long composite wind turbine blade under extreme loading. *Compos Struct* 246:112426